Forward-backward correlation and its incident energy dependence in secondary-electron emission from a thin carbon foil upon proton penetration

H. Ogawa,[1,*] A. Shimada,[2] M. Kiuchi,[2] M. Hagihara,[2] Y. Inoue,[2] K. Ishii,[1] and T. Kaneko[3]
[1]*Department of Physics, Nara Women's University, Nara 630-8506, Japan*
[2]*Graduate School of Humanities and Sciences, Nara Women's University, Nara 630-8506, Japan*
[3]*Graduate School of Science, Okayama University of Science, Okayama 700-0005, Japan*
(Received 16 February 2010; revised manuscript received 6 May 2010; published 29 July 2010)

The statistical distributions of the number of simultaneously emitted secondary electrons (SEs) from a carbon foil have been measured with proton beams of 0.5–3.5 MeV. In this experiment, the forward- and backward-emitted SEs have been measured simultaneously with foil-transmitted protons using a digitizer. As a method to examine how the forward and backward SE emissions correlate to each other, the forward (backward) SE yields γ_F (γ_B), that is, the mean number of the forward-emitted (backward-emitted) electrons per projectile, have been evaluated as a function of the number of the backward-emitted (forward-emitted) SEs, n_B (n_F). At higher incident energies, γ_F (γ_B) increases with increasing n_B (n_F). With decreasing incident energy, this so-called positive correlation becomes weaker and then changes to negative at the lowest incident energy. Although measurements using a slightly thicker foil exhibit just the same trend, the correlation changes from positive to negative at the higher incident energy. For a given foil thickness, the range of the produced binary electron and hence the incident proton energy seems to determine the sign of the correlation. A simple Monte Carlo simulation for the forward and backward SE emission in the present experimental condition can qualitatively reproduce the observed incident-energy dependence of the positive correlation but cannot reproduce the negative one observed at the lower incident energies.

DOI: 10.1103/PhysRevA.82.012902 PACS number(s): 79.20.Rf, 34.50.Bw, 34.50.Fa

I. INTRODUCTION

Kinetic emission of secondary electrons (SEs) from a solid surface under fast ion bombardments is one of the most fundamental and interesting phenomena in atomic collisions in solids and has been studied intensively for a long time [1,2]. It is established that this process can be described by the following three-step model: The first step is the creation of internal SEs via collisions of projectiles with target atoms in the solid. The second step is the transport of these electrons through the bulk to the surface including higher-order ionizations by δ-rays (i.e., SEs with high energies). The third step is to overcome the surface potential barrier [3]. As far as the light-ion incidence is concerned, the SE yields γ (i.e., the average number of the emitted electrons per projectile) are also known to be proportional to the electronic stopping power S_e of the target material [2–5]. This relation is quite reasonably understandable because the total energy per unit length deposited to the excited electrons produced in the first step should be proportional to the energy loss of the projectile.

The measurement of the electron emission statistics (i.e., the number distribution of emitted SEs per projectile) seems to be an effective method to investigate the detail of the ion-solids interaction. In particular, the simultaneous measurement of emitted SEs from both the beam-entrance and the beam-exit surfaces of a thin foil may bring about quite valuable information because the numbers of the forward- and backward-emitted SEs show a clear correlation in some cases (referred to as FB correlation hereafter), reflecting particular collisions of projectiles with target atoms. In this connection, this kind of measurement using carbon foils has been carried out by several authors with protons [6], heavy ions [7,8], and molecular ions [9]. For proton and hydrogen beams of the MeV region incident on a thin carbon foil, Smidts *et al.* [6] measured the numbers of the forward- and backward-emitted SEs simultaneously in coincidence with emergent protons. For the hydrogen incidence, they found a negative FB correlation; that is, the backward SE yield, γ_B, decreases with increasing number of the forward-emitted SEs. This behavior can be explained by the electron loss of the projectile hydrogens and the behavior of the lost electrons. If they undergo backscattering in the foil, they contribute mainly to the backward and not to the forward SE emission. This observation is also compatible with their own calculation using a Monte Carlo simulation [6]. On the other hand, γ_B are almost constant irrespective of the number of forward-emitted SEs for the proton incidence in coincidence with exiting protons. However, internal SEs produced by the incident protons can bring about a positive FB correlation if they have enough kinetic energy to produce other electrons over the whole depth of the foil through the cascading ionization. This situation can be realized when high-energy protons penetrate a thin carbon foil.

In the present work, the emission statistics of SE from a thin carbon foil in the forward and backward directions have been measured simultaneously with 0.5–3.5-MeV proton beams in coincidence with the foil-transmitted proton. The same measurements have been carried out using a couple of foils with slightly different thicknesses. From the obtained 2D (forward and backward) emission statistics, the mean number of forward-emitted (backward-emitted) electrons per projectile have been evaluated as a function of the number of the backward-emitted (forward-emitted) SEs. At higher

*ogawa@cc.nara-wu.ac.jp

incident energies, γ_{F,n_B} (γ_{B,n_F}) increases with increasing n_B (n_F). With decreasing incident energy, this positive FB correlation becomes weaker and finally changes to negative. For the thicker target foil, this change occurs at the higher incident energy. The observed behaviors are compared with simple model calculations using a Monte Carlo simulation. In this calculation, the incident protons were assumed only to excite plasmons, leading to low-energy electron production by their decay or to produce the binary electrons by collisions with individual electrons in the target foil. The binary electrons produced by the incident protons were assumed to create the plasmon or to be elastically scattered by the ion core of carbon atoms or to produce other binary electrons.

II. EXPERIMENT

The experiment was performed using proton beams obtained with a 1.7-MV tandem Van de Graaff accelerator at Nara Women's University. Measurements were carried out at proton energies from 0.5 to 3.5 MeV in 0.5-MeV steps. The collimated proton beams were transported to a target carbon foil with the same method described in our previous papers [10–13]. The target foil was tilted by 45° relative to the normal angle of incidence and floated at a potential of −30 kV. A couple of grounded electrodes were placed parallel to the beam entrance (backward) and exit (forward) surfaces of the foil and 40 mm away from the foil. The electrons emitted from the surfaces were accelerated to the corresponding electrodes and were detected by each solid-state Si detector with a 100 mm^2 sensitive area. The foil-transmitted protons were detected by a Si photodiode (PD) of 800 mm^2 sensitive area. The signals of forward- and backward-emitted electrons have been stored simultaneously together with the foil-transmitted particles with a digitizer. The thickness of the two carbon foils employed was determined to be 1.9 ± 0.1 $\mu g/cm^2$ and 2.5 ± 0.1 $\mu g/cm^2$ by measuring the transmitted fraction of 2.5-MeV H^0 particles, accounting for the electron loss and capture cross sections involved [14]. These values of thickness are those at the surface normal. During the SE measurement, the proton counting rate at the PD was kept to be 200–300 counts/s. At each incident energy, data were acquired until the total number of the foil-transmitted protons amounted to $\sim 2 \times 10^6$.

It should be mentioned that our measurements were carried out under a typical pressure of $\sim 2 \times 10^{-7}$ Torr, and no prior treatment of the target foil had been applied. As a consequence, the present data seem to include some effects from adsorbed contaminants. It is well known that the SE yields are very sensitive to the surface conditions of the foil [2]. On the other hand, the SE yields may also be affected by surface modifications induced by the incident beam. However, the coincidence measurement requires very low beam intensity, so the obtained results are expected to be free from such modifications. As a consequence, there might be some discrepancies between the present absolute values and those obtained with sputter-cleaned foils in an ultrahigh vacuum. But the relative changes of the SE emission such as the correlation of the forward- and backward-emitted SEs and its incident-energy dependence are expected to be sufficiently reliable.

III. DATA ANALYSIS

From the two-dimensional emission statistics of the forward- and backward-emitted SEs, the forward [backward] SE yields γ_F [γ_B] have been evaluated as a function of the number of the backward-emitted [forward-emitted] SEs n_B [n_F]. The data analysis was carried out in the same manner as employed in our previous work [13]. At first, we have selected such events that have an energy signal of the backward-emitted [forward-emitted] electrons within a narrow peak region corresponding to the simultaneous n_B [n_F] SE emission. For these events, the emission probability of n_F [n_B] electrons, $P_{n_B}(n_F)$ [$P_{n_F}(n_B)$], was derived with the same method mentioned in Refs. [10–12]. Finally, the forward [backward] SE yields gated by n_B [n_F] SE emission, γ_{F,n_B} [γ_{B,n_F}] is given as

$$\gamma_{F,n_B} = \sum_{n_F=1}^{n_{F,max}} n_F P_{n_B}(n_F), \tag{1}$$

$$\gamma_{B,n_F} = \sum_{n_B=1}^{n_{B,max}} n_B P_{n_F}(n_B), \tag{2}$$

where $n_{F,max}$ [$n_{B,max}$] denotes the maximum number of forward-emitted [backward-emitted] SEs per projectile observed in the spectra, typically 13–17.

IV. RESULTS AND DISCUSSION

Figure 1 denotes the results of the above-mentioned analysis for the target carbon foils of 1.9 ± 0.1 $\mu g/cm^2$. Figures 1(a) and 1(b) show the forward SE yields gated by the number of the backward-emitted SEs and vice versa, respectively. The values of γ_F (γ_B) for $n_B = 0$ ($n_F = 0$) are indicated with dotted lines as a guide. Associated errors were estimated from the statistical ones for the total numbers of events involved. As is clear from Fig. 1, γ_{F,n_B} (γ_{B,n_F}) increases with increasing n_B (n_F) at the incident energies above 1.0 MeV. This positive FB correlation appears more striking with increasing the incident energy. Incident protons produce not only low-energy electrons via distant collisions with target electrons but also binary electrons via close collisions with individual electrons. The binary electrons that have a range comparable to or larger than the foil thickness can bring about the positive FB correlation by cascading ionization. Since the average kinetic energy of produced binary electrons becomes higher with increasing proton energy, the observed trend is quite understandable qualitatively. On the other hand, the correlation changes to negative at 0.5 MeV. In this energy, the range of most binary electrons is so small that they cannot produce cascading electrons over the whole depth of the foil. In this connection, Iskef *et al.* have proposed a semiempirical range-energy relation of electrons applicable to all kinds of target materials [15]. According to this relation, the ranges of electrons with the same velocity as 0.5- and 1.0-MeV protons correspond to 1.4 and 3.3 $\mu g/cm^2$, respectively. These values are not inconsistent with the above interpretation of the observed FB correlation. If the range of the majority of the produced binary electrons becomes smaller than the thickness of the target foil, these electrons may contribute only to the

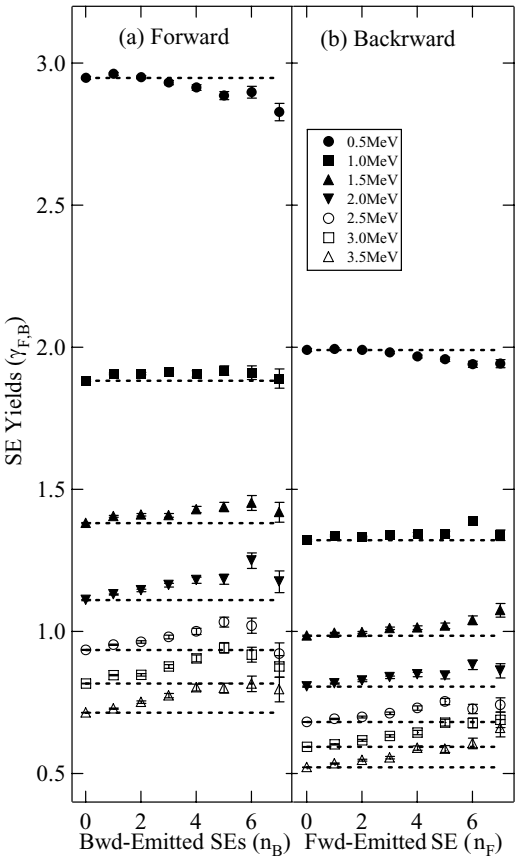

FIG. 1. The incident-energy dependence of the FB correlation measured in the SE emission from a carbon foil of 1.9 ± 0.1 μg/cm^2 thickness: (a) the forward SE yields, γ_F, gated by the number of backward-emitted SEs, n_B, and (b) the backward SE yields, γ_B, gated by the number of forward-emitted SEs, n_F. Horizontal lines are used as a guide to indicate the forward (backward) SE yields at $n_B = 0$ ($n_F = 0$).

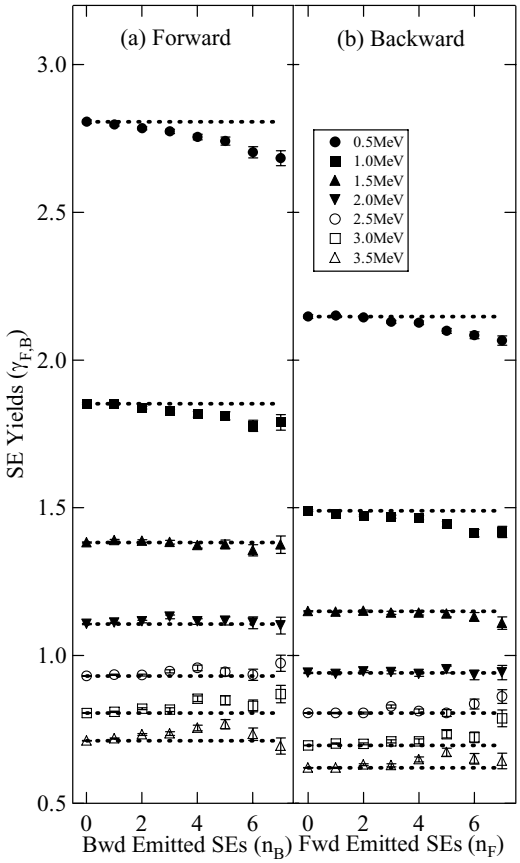

FIG. 2. Same as Fig. 1 except that the target carbon foil used is 2.5 ± 0.1 μg/cm^2 in thickness.

forward or the backward SE emission depending on the depth where they are created. For example, when regarding all of the target electrons as free and at rest, the mean free path (MFP) of the production of a binary electron which has a range larger than the foil thickness by a proton of 0.5 MeV is estimated to be four to five times larger than the foil thickness. On the other hand, a binary electron having a range of 0.8 μg/cm^2 is produced with a MFP equal to the foil thickness. Judging from these estimations, a proton of 0.5 MeV can produce at most one binary electron having a range larger than one third or half of the foil thickness and the probability of two or more high-energy binary electrons being produced is expected to be rather small. These situations are expected to be the origin of the observed negative correlation and, in the end, the target thickness seems to determine the threshold incident energy where the sign of the FB correlation changes.

In order to examine this prediction, the same measurements have been carried out with another carbon foil of 2.5 ± 0.1 μg/cm^2 thickness. The obtained values of γ_{F,n_B} and γ_{B,n_F} are presented in Fig. 2. Usually the SE yields increase with increasing foil thickness in the present foil-thickness region [3,5,10], while the γ_{F,n_B} values given in this figure are smaller than the corresponding ones for the thinner foil at each energy. This may be due to the difference of the surface condition between the two foils. As mentioned above, however, this difference is expected not to affect the FB correlation and its incident-energy dependence discussed here. Also for this foil, a similar incident-energy dependence of the FB correlation appears except that the correlation changes from positive to negative around 2.0 MeV. This result appears to support the above explanation of the negative FB correlation observed in the present results.

In order to understand the mechanism, we have calculated the number distribution of the forward- and backward-emitted SEs under the present experimental condition using a Monte Carlo simulation. At first, incident protons are assumed to penetrate the foil by repeating plasmon excitations and binary collisions with target electrons. The MFP of the plasmon excitation by an incident proton, λ_{pl}, is calculated using a dielectric-function method for a damped plasmon with the decay constant [16]. In binary collisions, target electrons are treated as free and at rest. According to this simplification, the impact parameter b between an incident proton and a target electron determines the recoil velocity v_e and angle ϕ of the produced binary electron as

$$b = \frac{e^2}{m_e v^2}\left(\frac{2v^2}{v_e^2} - 1\right)^{1/2} = \frac{e^2}{m_e v^2}\tan\phi, \qquad (3)$$

where e, m_e, and v denote the elementary charge, electron mass, and projectile velocity, respectively. From Eq. (3), the

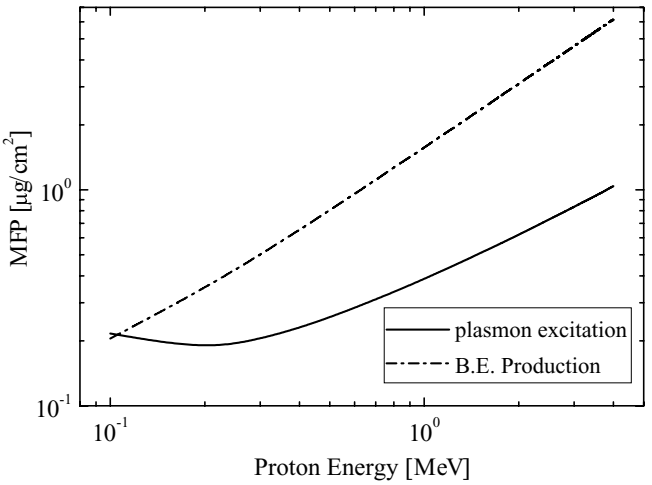

FIG. 3. The MFPs of the protons in a carbon foil employed in the present Monte Carlo simulation are represented for the plasmon excitation and the binary electron production as a function of the incident energy. For the binary electron production, target electrons are treated as free and at rest, and the minimum recoil velocity of created binary electrons, $E_{\mathrm{BE,min}}$, is taken to be twice that of the Bohr velocity, v_{B}.

minimum velocity of the produced binary electron, $v_{\mathrm{BE,min}}$, sets the maximum impact parameter and hence the MFP of the binary electron production, λ_{BC}. This velocity, therefore, the minimum kinetic energy of created binary electrons, $E_{\mathrm{BE,min}}$, is one of the free parameters in the present simulation. It seems that at least, a value comparable to or larger than the binding energies of L-shell electrons in a carbon atom, 10–20 eV, should be selected [17]. Therefore, in the present calculation, $v_{\mathrm{BE,min}}$ is set to be twice that of the Bohr velocity, v_{B}. In this connection, it has been confirmed that a simulation taking $v_{\mathrm{BE,min}} = 3v_{\mathrm{B}}$ does not significantly change the essence of the incident-energy dependence in the FB correlation.

In Fig. 3, the MFPs of incident protons in a carbon foil employed in the present Monte Carlo simulation are represented for the plasmon excitation and the binary electron production as a function of the incident energy. The MFP is given in units of $\mu\mathrm{g/cm}^2$. The total MFP of an incident proton, $\lambda_{p,\mathrm{tot}}$, is given as

$$\frac{1}{\lambda_{p,\mathrm{tot}}} = \frac{1}{\lambda_{\mathrm{BC}}} + \frac{1}{\lambda_{\mathrm{pl}}}. \tag{4}$$

A pseudorandom number generated in the computer determines the depth where an incident proton is subjected to the first collision in the foil. Using another pseudorandom number, the type of the collisions (i.e., the plasmon excitation or the binary electron production) is selected. If binary electron production is selected, the impact parameter, the recoil energy, and the recoil angle of the binary electron are determined with this pseudorandom number. The azimuthal angle of the binary electron is determined with the next pseudorandom number. Next, binary electrons produced directly by incident protons (which we call primary electrons) penetrate the foil by repeating (a) plasmon excitations, (b) scatterings by the Bohr-type screened Coulomb potential of carbon nuclei [18], and (c) production of other binary electrons. As for the plasmon excitation, the MFP for an electron is assumed to be equal to that for a proton of the same velocity. For process b, the maximum impact parameter and hence the MFP of the scattering can be obtained from the minimum scattering angle, θ_{min}, using an analytical relation between the impact parameter and the scattering angle. In the present calculation, θ_{min} is taken to be $\pi/16$ rad. Since the screened Coulomb potential is employed, a calculation with the smaller θ_{min} gives almost the same result. For the binary electron production by primary electrons, target electrons are regarded to be free and at rest and the cascade multiplication (CM) is taken into account up to second order; that is, the production of "daughter" and "granddaughter" electrons by primary ones are considered. The minimum energy $E_{\mathrm{CM,min}}$ of the daughter and granddaughter electrons produced by the collisions of a couple of electrons is also a free parameter in our simulation. In test calculations with 10 and 20 eV for $E_{\mathrm{CM,min}}$, the results did not differ so much from each other and the former value was employed. From this value, the maximum impact parameter for the electron-electron collision and hence its MFP is determined.

Figure 4 represents the MFPs in units of $\mu\mathrm{g/cm}^2$ for these three processes as a function of the electron energy. The total MFP of a binary electron can be given in a similar manner to that of the proton except that three competing processes are considered. The method to determine the distance between two successive collisions, the type of the collision, the impact parameter, and so forth is quite similar to that for the incident protons. For the binary electrons, however, their energy losses were taken into account by subtracting the product of the path length between the two successive collisions and the stopping power calculated with the dielectric-function method [16].

In order to calculate the position where the binary electrons suffer collisions in the foil-fixed frame, Euler angles are introduced. When a binary electron is produced or suffers backscattering, the coordinates are transformed so that the

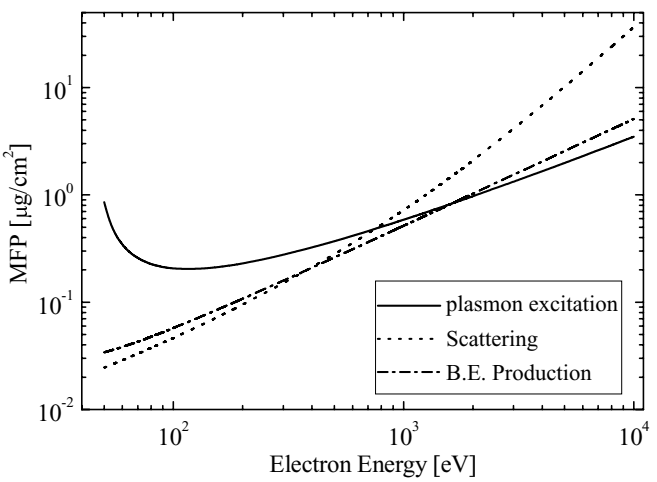

FIG. 4. The MFPs of binary electrons in a carbon foil employed in the present Monte Carlo simulation are represented for the plasmon excitation, the scattering by the carbon nucleus, and the production of other binary electrons as a function of the electron energy. As for the scattering, the minimum scattering angle, θ_{min}, was taken to be $\pi/16$ rad. For the binary electron production, target electrons are treated as free and at rest, and the minimum energy of the created electrons, $E_{\mathrm{CM,min}}$, is taken to be 10 eV.

binary electron moves on the "new" z axis. When the cascade multiplication occurs, a couple of new z axes are assigned. The behavior of a binary electron is pursued until it reaches outside the foil or its kinetic energy becomes smaller than a threshold energy, $E_{e,\min}$. Binary electrons leaving the foil and depositing a part of their kinetic energy in it have also been counted as forward- or backward-emitted SEs. As explained below, binary electrons slower than $v_{\mathrm{BE},\min}$ but having a kinetic energy larger than the threshold energy, $E_{e,\min}$, are treated in the same manner as electrons generated by the decay of the plasmon. A practical value of $E_{e,\min}$ is equated to that of $E_{\mathrm{CM},\min}$, 10 eV.

If a plasmon is excited by an incident proton or by a binary electron, it decays to an electron-hole pair. Then, an electron is assumed to be liberated at just the same position. The contribution of this electron to the SE emission is simulated based on the following assumption. At first, the distance to the forward and backward surfaces are calculated and the electron is assumed to diffuse toward the closer surface. The electron arriving at the surfaces can escape to vacuum when it has energy enough to overcome the surface potential barrier. These processes are characterized by the diffusion length for low-energy electrons, λ_S, and the surface transmission probabilities, P_B and P_F, for beam-entrance and -exit surfaces, respectively [3,5]. In the present calculation, the value of λ_S is taken to be 0.85 μg/cm^2, which was obtained in our previous work [10]. Although the γ_F (γ_B) is proportional to P_F (P_B), we are concerned with the FB correlation and its incident-energy dependence rather than the absolute values of γ_F or γ_B. Therefore, the values of P_F and P_B are taken to be 0.48 and 0.37, respectively, so that the simulated forward and backward SE yields agree with those obtained in the present experiment at 2.5 MeV for the thinner target foil. The same values are used at other incident energies and also for the thicker foil. Throughout the simulation, daughter and granddaughter electrons were treated the same as primary ones, besides the fact that daughter electrons can produce another binary electron only once and that granddaughter ones

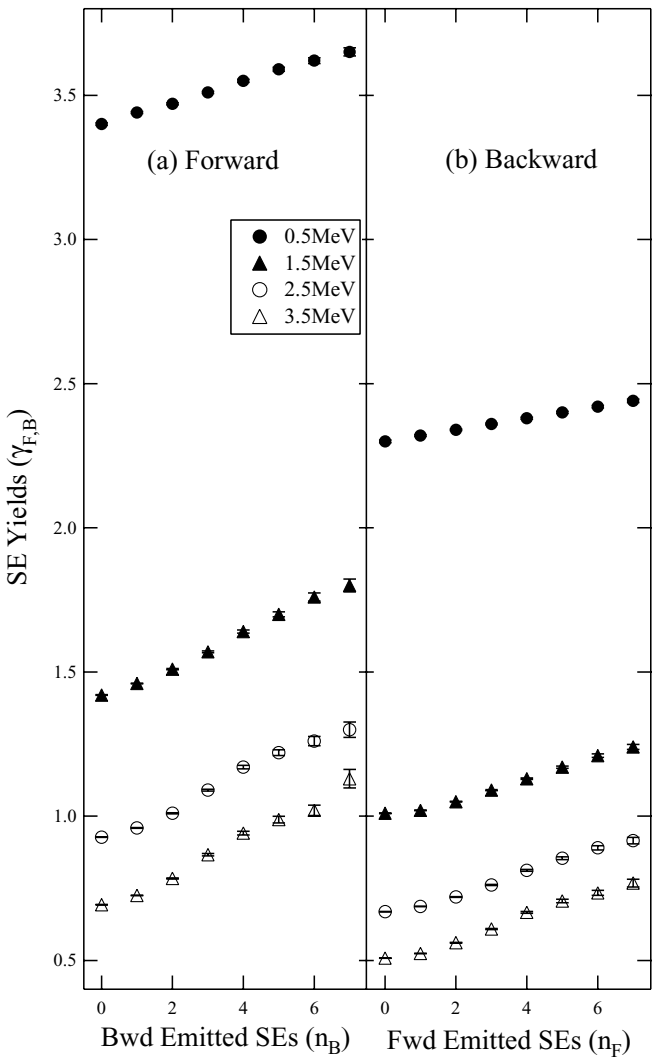

FIG. 5. Results of a Monte Carlo simulation for the FB correlation in the SE emission from a carbon foil of 1.9 ± 0.1 μg/cm^2 thickness: (a) forward SE yields, γ_F, gated by the number of backward-emitted SEs, n_B, and (b) backward SE yields, γ_B, gated by the number of forward-emitted SEs, n_F. Since the positive FB correlation becomes weaker monotonically with decreasing incident energy for both γ_F and γ_B, results of the simulation are given only at every 1-MeV step from 0.5 MeV.

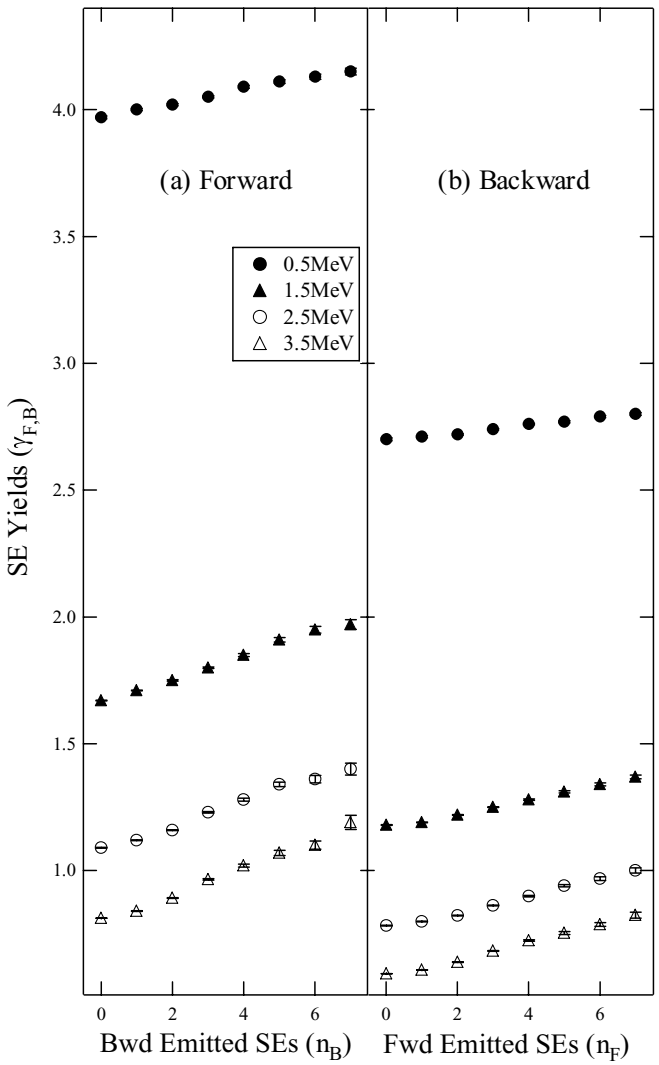

FIG. 6. Same as Fig. 3 except that the target carbon foil is 2.5 ± 0.1 μg/cm^2 in thickness.

cannot. The simulation was carried out for a total number of 1×10^7 foil-transmitted protons at each energy. Before presenting the result of the simulation and comparing with the experimental data, we briefly mention the contribution from each process, the plasmon excitation by the incident protons, primary and cascaded binary electrons, those slowing down below the threshold energy $E_{e,\min}$, and so forth obtained by the simulation for the incident energy of 0.5 MeV, where the negative FB correlations are observed experimentally for both of the target foils. At first, the relative contributions from the plasmons produced by protons are 43% and 49% in the forward and backward SE yields, respectively. Of course, these SEs exhibit no FB correlation. Electrons from plasmons produced by binary electrons occupy 18% and 16% in the forward and backward directions, respectively, and these correlate strongly with each other. Those slowing down below $E_{e,\min}$ have a contribution of 32% in both directions. Although they are originally primary, daughter, or granddaughter electrons, they have no correlation. Binary electrons leaving the foil and depositing a part of their kinetic energy in it are 7% and 3% in the forward and backward directions and those originating from the cascade multiplication exhibit the FB correlation.

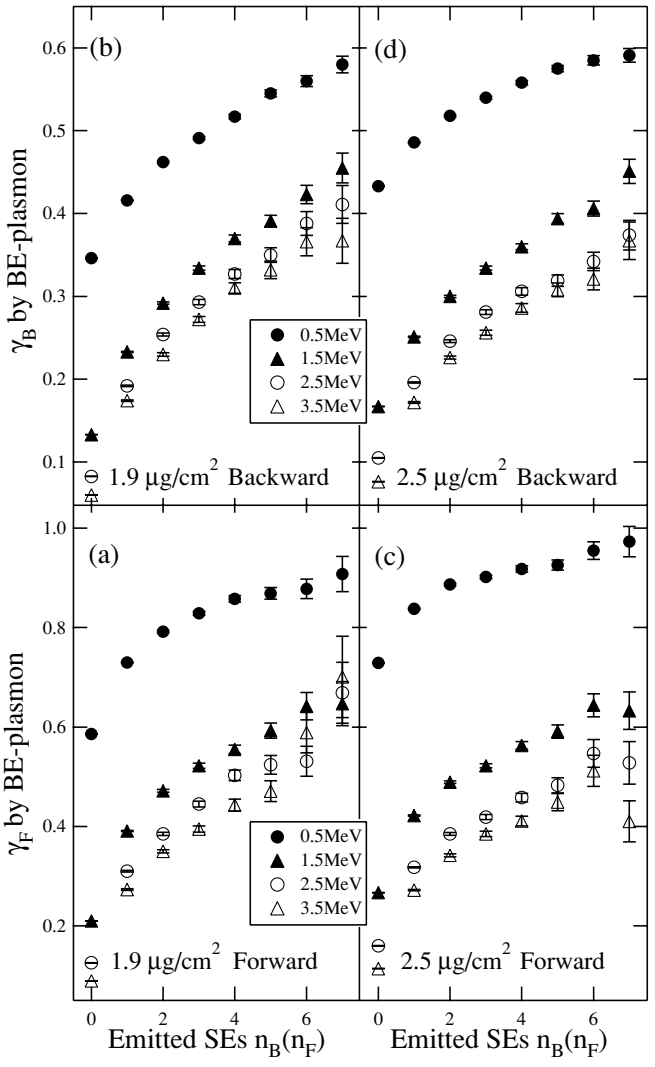

FIG. 7. The contribution of SEs from plasmons produced by binary electrons to γ_F and γ_B gated by the number of those emitted at the opposite surface: (a) γ_F and (b) γ_B gated by n_B and n_F for the thinner foil, respectively, and (c, d) those for the thicker foil.

Figures 5 and 6 represent the results of the simulation for target foils of 1.9 and 2.5 μg/cm^2 thickness, respectively. Calculations can qualitatively predict the incident-energy dependence of the observed positive FB correlation, that is, the decrease of the correlation with decreasing the incident energy. Above 2.5 MeV, the positive correlation becomes weaker for the thicker target foil. This trend is also compatible with the observed one. However, the negative correlation observed clearly in the experimental data at the lower energy cannot be reproduced. As mentioned above, electrons from plasmons produced by binary electrons in the forward and backward directions correlate strongly with each other.

Figure 7 represents the contribution of these electrons obtained by the simulation. Figures 7(a) and 7(b) show the results of γ_F gated by n_B and of γ_B gated by n_F for the thinner foil, 1.9 μg/cm^2, respectively. Figures 7(c) and 7(d) are those for the thicker foil, 2.5 μg/cm^2. Contrary to our expectation, electrons from plasmons produced by binary electrons also exhibit a positive FB correlation even at the lowest incident energy. In some points, however, our simulation may oversimplify the collision processes which the incident protons and the binary electrons produced by them induce in the foil. For example, the binding energies of the target electrons are ignored. Cascade multiplications of binary electrons of third and higher orders are also neglected. In order to reproduce the negative FB correlation, a more sophisticated calculation may be inevitable.

V. CONCLUSIONS

The correlation between the forward- and backward-emitted SEs from carbon foils by penetration of 0.5–3.5-MeV proton beams has been investigated by measuring the number distributions of SEs in both directions simultaneously. With decreasing incident energy, the positive FB correlation observed at higher energy becomes weaker and then changes to a negative one. By comparing the results for a couple of foils with different thicknesses, it is found that this change occurs at higher energy for the thicker foil. Experimental results are compared with calculations by a simple Monte Carlo simulation assuming that incident protons excite plasmons and binary electrons followed by their plasmon excitations, scatterings by the screened Coulomb potential of carbon nuclei, and other binary electron productions by cascade multiplication. Although the observed incident-energy dependence of the positive FB correlation can be reproduced qualitatively by the simulation, the negative one observed at the lower incident energy cannot be reproduced and is left to be clarified.

ACKNOWLEDGMENTS

The authors would like to acknowledge J. Karimata for his assistance in the operation of the accelerator. We would also like to thank H. Obata and M. Yasuda for their help in the experiment. One of the authors (T.K.) is grateful for partial support of a Grant-in-Aid for Scientific Research (C) from the Japan Society for the Promotion of Science.

[1] J. Devooght, J. C. Dehaes, A. Dubus, M. Cailler, J. P. Ganachaoud, M. Rősler, and W. Brauer, in *Particle Induced Electron Emission I*, edited by G. Höhler and E. A. Niekisch, Springer Tracts in Modern Physics, Vol. 122 (Springer, Berlin, 1991).

[2] D. Hasselkamp, H. Rothard, K. O. Groeneveld, J. Kemmler, P. Varga, and H. Winter, in *Particle Induced Electron Emission II*, edited by G. Höhler and E. A. Niekisch, Springer Tracts in Modern Physics, Vol. 123 (Springer, Berlin, 1991).

[3] E. J. Sternglass, Phys. Rev. **108**, 1 (1975).

[4] J. Schou, Scanning Electron Microsc. **2**, 607 (1988).

[5] H. Rothard *et al.*, Phys. Rev. A **51**, 3066 (1995).

[6] O. F. Smidts, A. Dubus, Z. Vidović, A. Billebaud, M. Fallavier, R. Kirsch, J.-C. Poizat, J. Remillieux, and M. Räosler, Nucl. Instrum. Methods B **157**, 239 (1999).

[7] A. A. Kozochkina, V. B. Leonas, and M. Witte, Nucl. Instrum. Methods B **62**, 51 (1991).

[8] Y. Yamazaki, K. Kuroki, T. Azuma, K. Komaki, H. Watanabe, N. Kakutani, T. Hasegawa, M. Sekiguchi, and T. Hattori, Phys. Rev. Lett. **70**, 2702 (1993).

[9] T. Azuma, Y. Yamazaki, K. Komaki, T. Hasegawa, T. Hattori, and K. Kuroki, Nucl. Instrum. Methods B **67**, 636 (1992).

[10] H. Ogawa, H. Tsuchida, M. Haba, and N. Sakamoto, Phys. Rev. A **65**, 052902 (2002).

[11] H. Ogawa, H. Tsuchida, and N. Sakamoto, Phys. Rev. A **68**, 052901 (2003).

[12] H. Ogawa, N. Fujimoto, T. Ohata, M. Nagano, K. Ishii, N. Sakamoto, and T. Kaneko, Nucl. Instrum. Methods B **256**, 532 (2007).

[13] H. Ogawa, M. Sonoda, Y. Inoue, K. Ishii, and T. Kaneko, Nucl. Instrum. Methods B **267**, 2612 (2009).

[14] H. Ogawa, N. Sakamoto, and H. Tsuchida, Nucl. Instrum. Methods B **164-165**, 279 (2000).

[15] H. Iskef, J. W. Unningham, and D. E. Watt, Phys. Med. Biol. **28**, 535 (1983).

[16] T. Kaneko, H. Kudo, S. Tomita, and R. Uchiyama, J. Phys. Soc. Jpn. **75**, 034717 (2006).

[17] J. P. Desclaux, At. Data Nucl. Data Tables **12**, 311 (1973).

[18] N. Bohr, Mat. Fys. Medd. K. Dan. Vidensk. Selsk. **18**, 8 (1948).